PROPERTIES OF NANO AND MICRO P-TYPE Cu$_2$S FILMS

HS Soliman[1], MM Saadeldin[2], K Sawaby[2] and *A Eldenglawey[3,4]

[1]Department of Physics, Faculty of Education, Ain-Shams University, Cairo, 11757, Egypt
[2]Department of Physics, Faculty of Science, Cairo University, Giza 12613, Egypt
[3]Nano and Thin film Lab. Department of Phys., Fac. of Sci., South Valley University, Qena, 83523, Egypt
[4]Department of Physics, Faculty of Applied Medical Sciences, Taif University, Turabah, 21995, KSA

ABSTRACT

Thermal evaporation technique under pressure 10^{-6} torr is used to prepare Cuprous Sulphide (Cu$_2$S) with different thicknesses on glass substrates. Energy dispersive X-ray (EDX), X-ray diffraction, scanning electron microscope (SEM), and atomic force microscope (AFM) are used to characterize the chemical composition and the structure of Cu$_2$S. The dark dc electrical resistivity (ρ) is measured using two point probe method at different temperatures (from 303 to 423 K). The thermoelectric power (Seeback coefficient) was investigated in temperature range (303 – 373 K).

Keywords: Cu$_2$S alloys, structural and electrical properties, thin films, thermal evaporation, XRD, SEM, AFM.

INTRODUCTION

Due to its lower cost preparation and the widest application through modern technology, semiconductor alloys has a great interest. Cu alloys could be used as a solar cell absorber due to their high solar conversion. It was reported that copper and sulfur have different phases, Copper Sulfide or Cu$_2$S is one of them (Grozdanove and Najdoski, 1995). Cu$_2$S is one of the promised materials due the highest electrical conductivity and its unique characteristics (Su *et al*., 2013; Abdel Rafea *et al*., 2012).

Cu$_2$S has direct and indirect band gap energy at 1.2eV and 1.8 eV respectively (Li *et al*., 2013). Nano crystalline Cu$_2$S thin films are used in many practical applications such as photovoltaic cells, tubular solar collections, automobiles glazing, solar control, coatings, gas sensors and photodetectors. Different techniques were reported (Su *et al*., 2013; Li *et al*., 2013; Dongol *et al*., 2012a; Li *et al*., 2014) to deposit cuprous sulphide thin film; thermal evaporation, sputtering, spray pyrolysis, chemical vapor deposition, solvo thermal method and successive ionic layer adsorption etc. Among of these available techniques, thermal evaporation was to deposit Cu$_2$S films.

MATERIALS AND METHODS

99.99% purity of powder cuprous sulphide, Cu$_2$S supplied

---

*Corresponding author e-mail: denglawey@lycos.com

by sigma Aldrich Company was used to prepare different thickness of Cu$_2$S films on glass substrates using a high vacuum coating unit (Edwards type E306A) under vacuum of 10^{-6} torr at room temperature. Powder is placed in a quartz crucible heated by tungsten coil to evaporate Cu$_2$S material. FTM5 quartz crystal monitor was used to control the evaporation rate (0.3 nm/s) and film thickness. Interferometry method was used to check the film thickness (Tolansky, 1988). Structural investigation was done using X-ray diffraction, XRD Philips X-ray diffractometer (model X0 Pert) of utilizing monochromatic CuKa radiation operated at 40 kV and 30 mA, scanning electron microscope (Philips XL30) attached with the EDX unit, scanning electron microscope (SEM, JEOL JSM-5500, Japan) with accelerating voltage 10 kV, Atomic force microscope, AFM-Shimadzu scanning probe microscope SPM-9500J3 and transmission electron microscope, TEM, JEOL.JEM,1010-Japan) with accelerating voltage 60 kV. More details of film preparation are available at (Dongol, 2012b). Electrical measurements was done using co-planar geometry. Metal mask was used to obtain inter-electrode gap of 2 mm width.

RESULTS AND DISCUSSION

EDX analysis' is used to check the chemical composition of the Cu$_2$S powder and thin film as depicted in figures 1 and 2. The results confirms that the produced material consists of both Cu and S with elemental ratio close to 2:1, this is agree with the stoichiometric ratio of Cu$_2$S (Li

et al., 2013). The elemental composition of Cu_2S, powder and thin film are listed in the table 1.

Table 1. Powder and thin film chemical composition of Cu_2S material.

Cu_2S Material	Cu%	S%	Chemical formula
Powder	87.27	12.73	Cu_2S
Thin film	72.63	27.37	$Cu_{1.96}S$

The XRD patterns of the as prepared and annealed films of Cu_2S are shown in figures 3 and 4. The obtained results indicated that the material is polycrystalline in nature. XRD of the as prepared films contains many diffraction lines existed with a broad hump at 2θ: 23.97, 24.90, 28.18, 30.41, 37.57, 43.46 and 48.58º with preferred orientations: (320), (260), (104), (360), (382), (111) and (346) as depicted in figure 3. Thus the as prepared film exhibits nano crystalline as well as polycrystalline nature. Full width half maximum (FWHM) of XRD scans of the
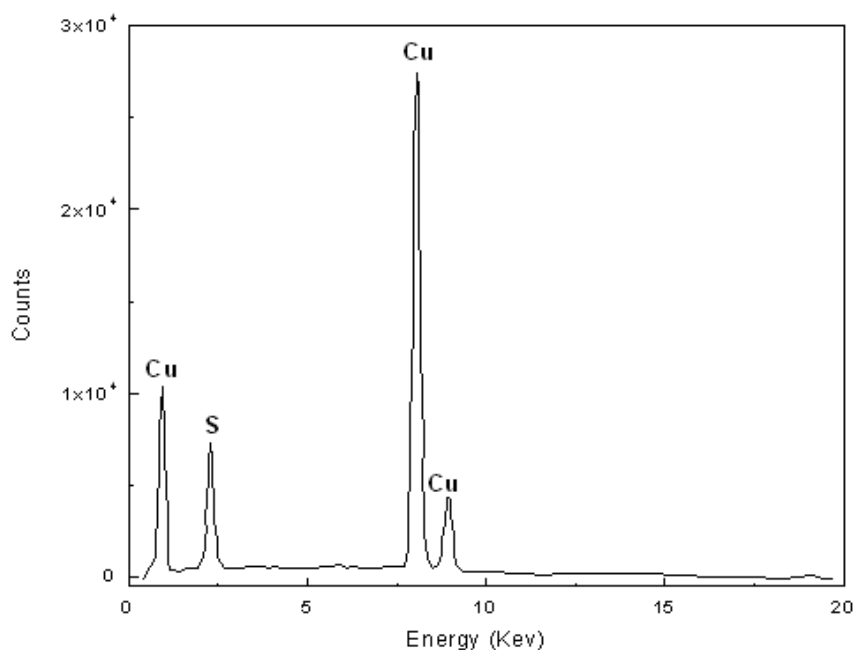

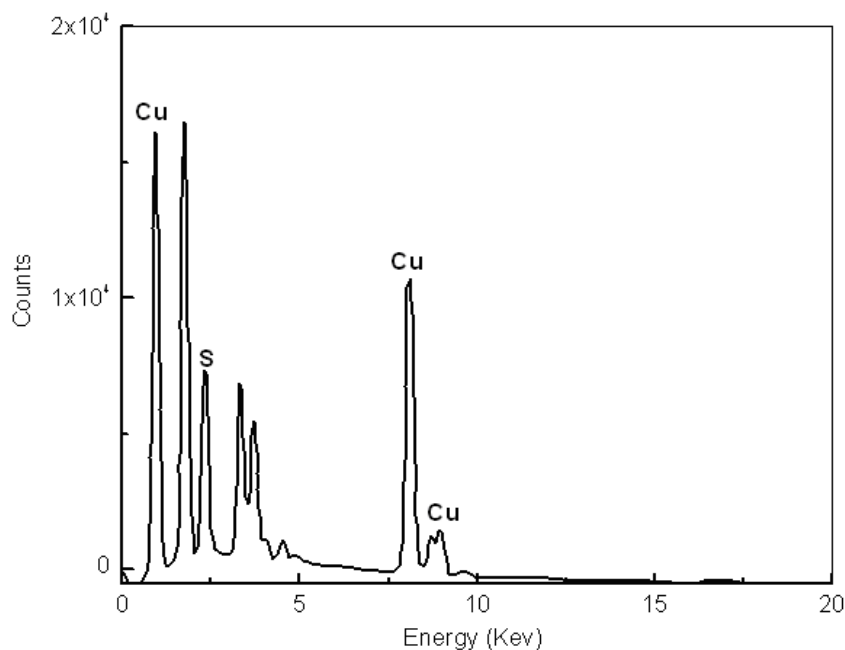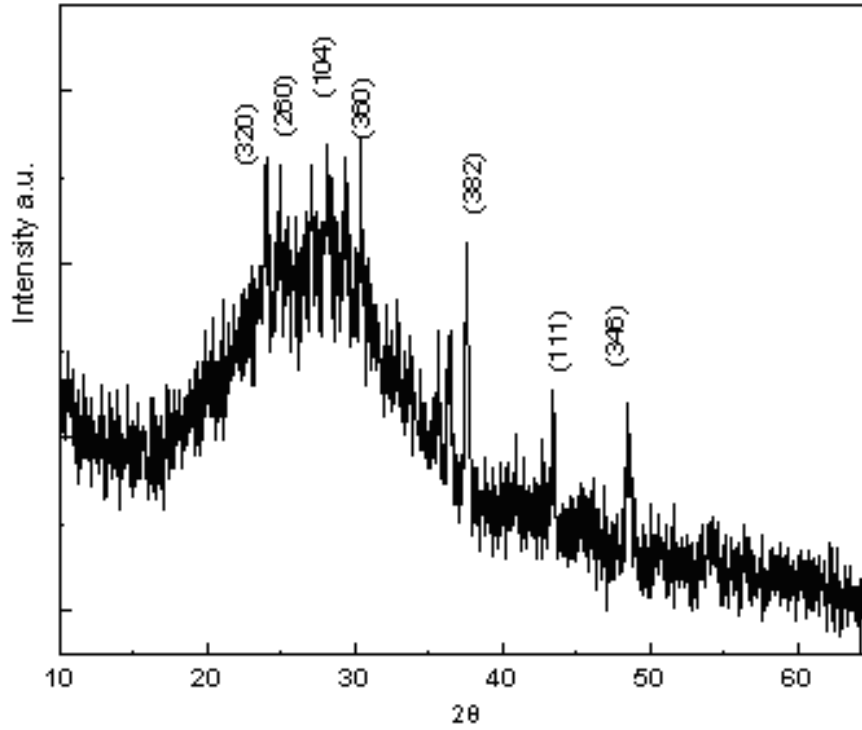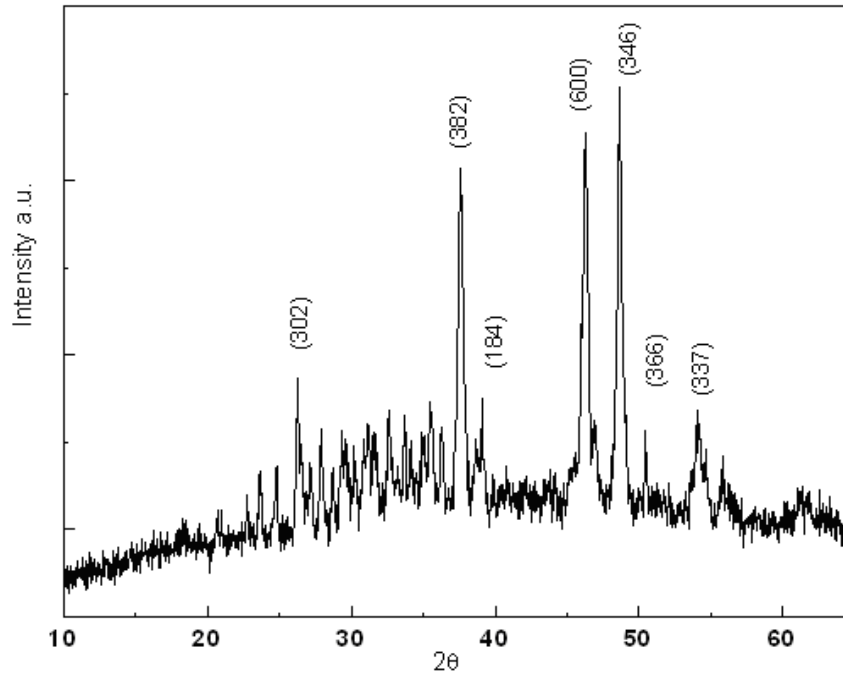Fig. 1. EDS distribution of the constituent of the elements Powder Cu_2S.

Fig. 2. EDS of Cu_2S films.

Fig. 3. XRD of Cu$_2$S films.

Fig. 4. XRD of annealed Cu$_2$S films.

as prepared and annealed Cu$_2$S films is used to calculate the crystallite size according to Sherrer equation (Varin *et al*., 1999).

$$D = \frac{K\lambda}{\beta\cos\theta} \qquad (1)$$

θ is the Bragg angle, λ is the wavelength of X-ray used (CuKα radiation) equal to 1.54056 A°, D is the crystallite size, and K is the shape factor, which is approximately unity. The calculated crystallites size corresponding to the mentioned preferred orientations of the as prepared films is 31, 21, 42, 34, 19, 40 and 25 nm, respectively. Due to annealing at 423K, many peaks are observed at 2θ;
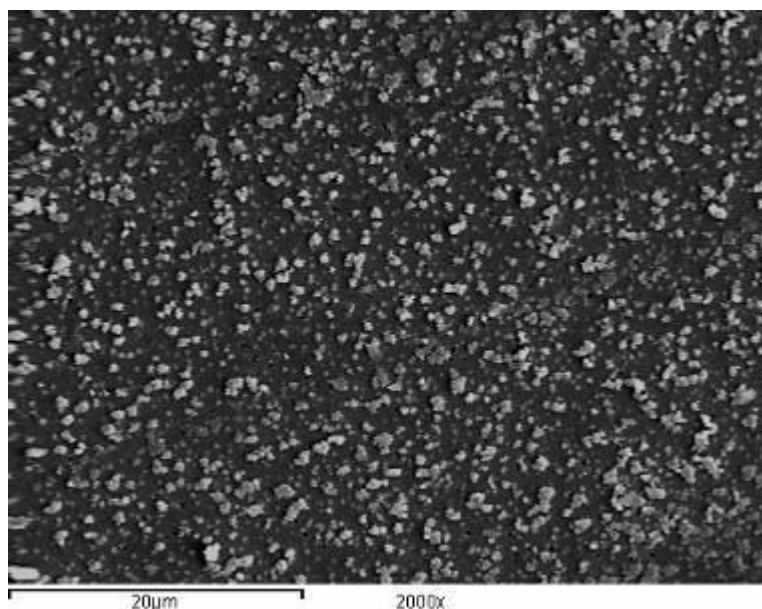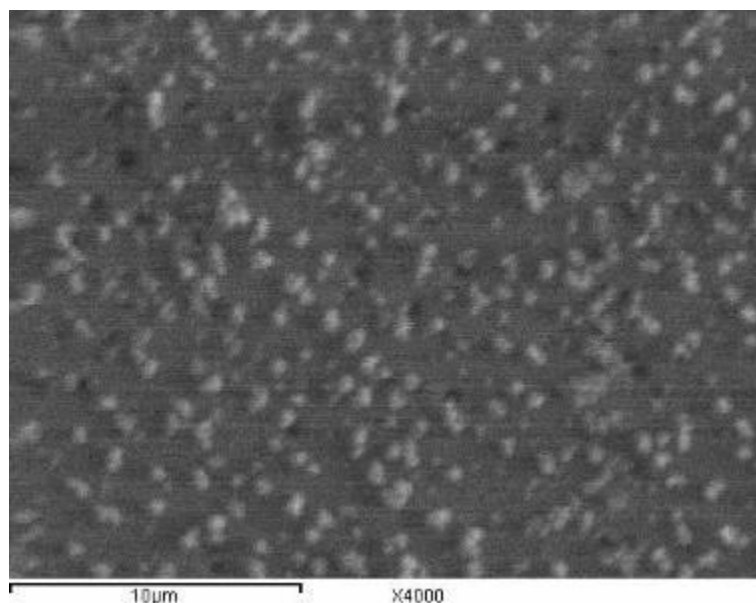
Fig. 5. SEM of the as prepared Cu₂S films.

Fig. 6. SEM of annealed Cu₂S films.

26.27, 37.62, 46.28, 48.66, 50.43, 54.14 and 55.78° with preferred orientations; (302), (382), (184), (600), (346), (366) and (337). The corresponding crystallites size is 45, 29, 20, 24, 163, 15 and 347 nm. The crystallite size of the preferred orientation (382) increases by the increasing of annealing temperature confirming the enhancement of crystallization. The obtained values of D confirm that the nano structure is approximately valid. The obtained data was augmented by (Ohtani *et al*., 1995; Carvalho *et al*., 2013; Shinde, 2013). The observed inter planar spacing; d_{hkl} was compared with the data of ICCD card No-09-0328. The indexing was carried out for the patterns, and their peaks were identified for orthorhombic crystal system with lattice parameters: $a = 11.82$ A^0, b = 27.05 A^0 and $c = 13.43$ A^0.

Surface morphology of the as deposited and annealed (423 K) Cu₂S films was investigated by the scanning electron microscopy (SEM). The SEM image of the as-deposited Cu₂S thin films is shown in figure 5. It reveals that the deposited film covers the substrate well consequently uniform distribution and characterized by nano crystallites within range 12 -420 nm. It is known
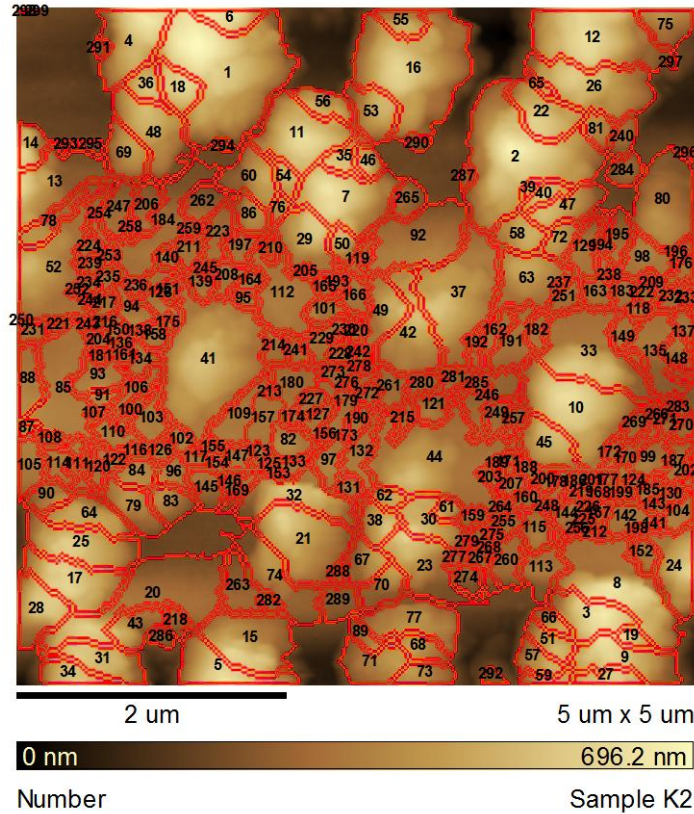
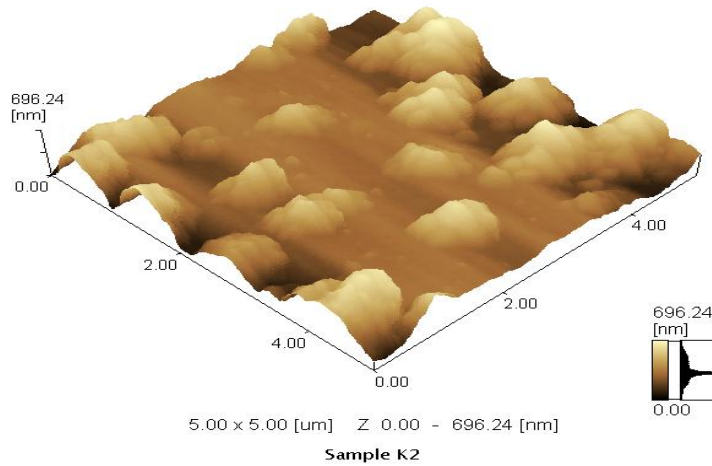Fig. 7-a. AFM micrograph of crystallite size of as-prepared Cu₂S films.

Fig. 7-b. 3D AFM micrograph of surface morphology of as-prepared Cu₂S films.

that the growth of the crystallites plays a great role in the shape of sample morphology and the crystal growth of some preferred structure or planes are related to the surface energy of the planes in the specified condition, figure 6 shows the surface morphology of the annealed film. The granular like crystallites are observed with higher size compared with the as prepared film, which indicates the crystallite size is increased by annealing confirming the increasing of homogeneity, consequently morphology (Shinde *et al*., 2013).

AFM measurements is performed on both as prepared and annealed films with scan area 5 μm X 5 μm as shown in figure (7.a), (7.b), figure (8.a) and (8.b), respectively.
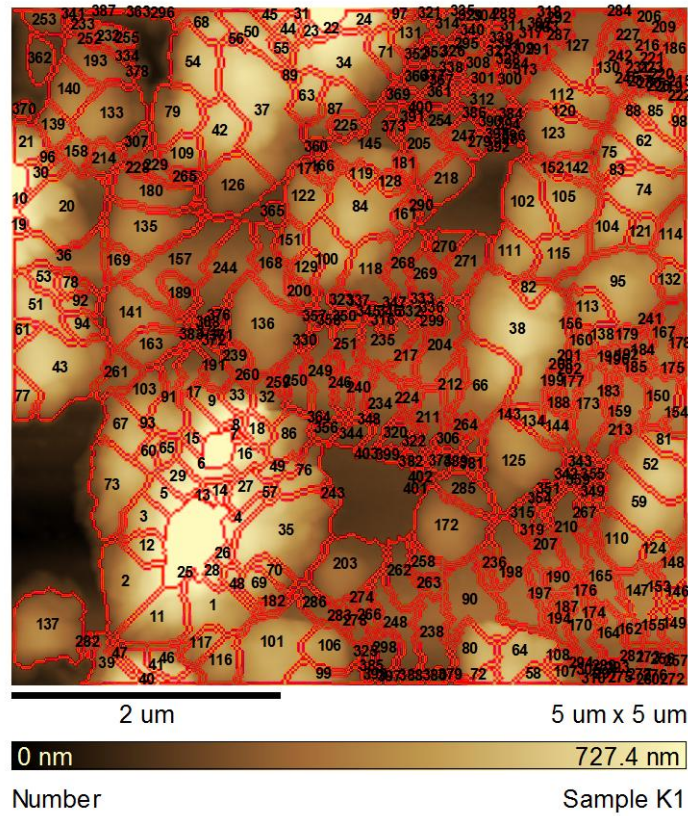
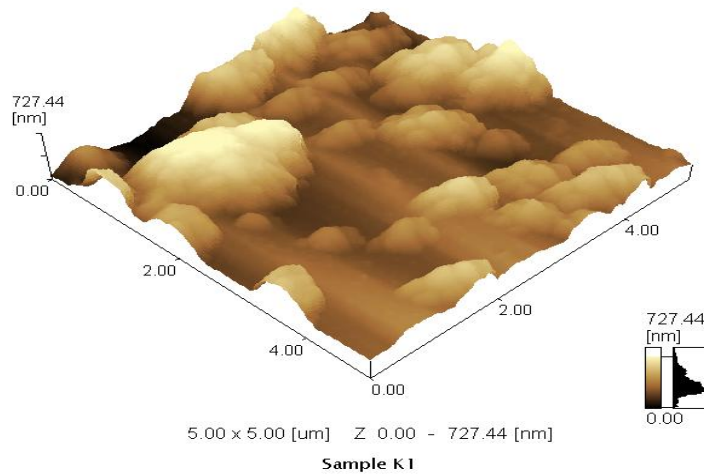Fig. 8-a. AFM micrograph of crystallite size of annealed Cu$_2$S films.

Fig. 8-b. 3D AFM micrograph of surface morphology of annealed Cu$_2$S films.

The mean radius and roughness of the crystallites is measured by computer programming.

Both mean radius and roughness of the films increase with annealing temperature; 107, 1.58 -125, 1.8 nm respectively.   The crystallization at 423K causes the growth of the larger crystallite with different sizes responsible for the increasing of roughness (Carvalho, 2013; Lewkowicz, 2014; Abdel Rafea et al., 2012). The crystallite sizes range in case of as prepared and annealed films are (1-289) and (1-402) nm, respectively.
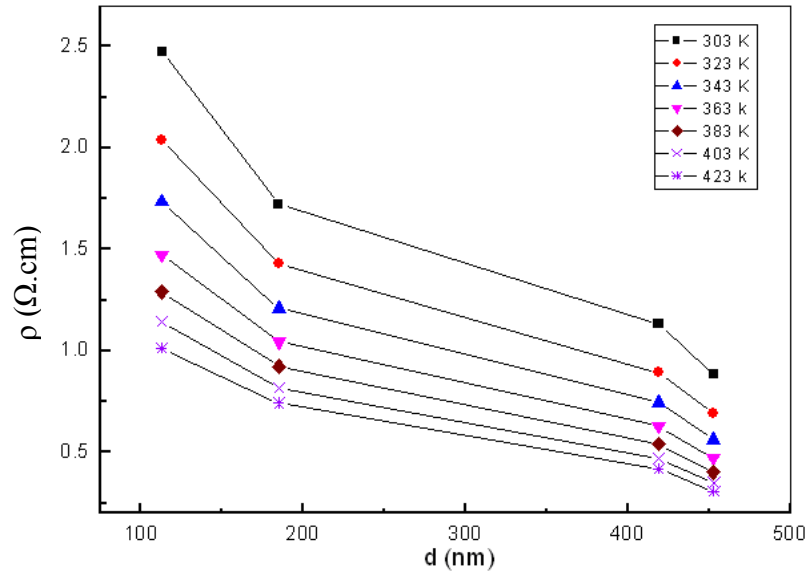
Fig. 9. Dependence of dark resistivity of Cu_2S films on the films on thickness at different annealing temperatures.
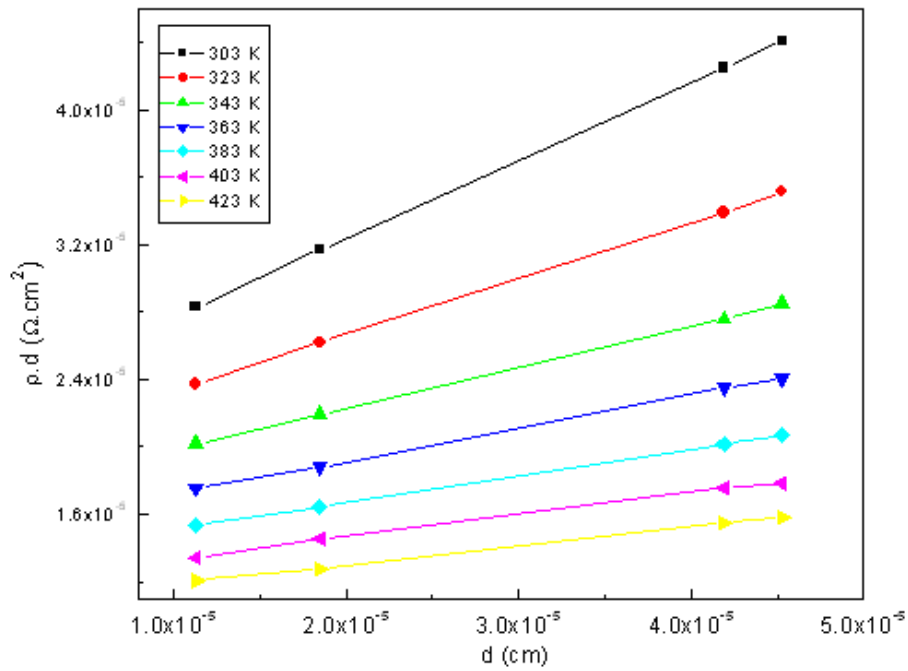

Fig.10. Dependence of dark resistivity of Cu_2S films on the film thickness at different annealing temperatures.

The range difference of the value of crystallite size that calculated from XRD, SEM and AFM may be attributed to the different proposed techniques (Salim *et al.*, 2011).

Electrical characterization
The dark electrical resistivity, ρ is calculated for Cu_2S films of different thicknesses; 113, 185, 419 and 453 nm within temperature range of 303-423 K according to:

$$\rho = R\frac{Wd}{L} \tag{2}$$

Where, W is width of the film , d is the thickness of the film and L is the length of the film. More details of the evaporation process and film thickness measurements are available at ELdenglawy (2005).

Figure 9 shows the variation of dark electrical resistivity as a function of film thickness at different temperatures. As illustrated the resistivity decreases with increasing film thickness in accordance with the typical results for the semiconducting films [Dhumure and Lokhands, 1992].
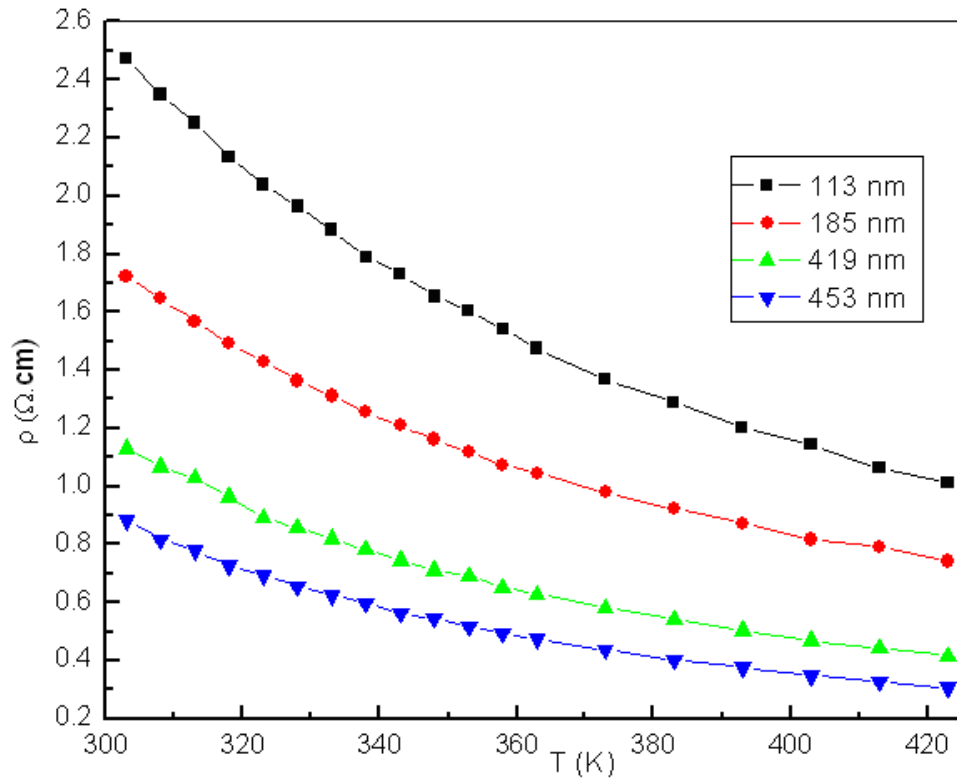
Fig.11. Dependence of dark resistivity of Cu_2S films on annealing temperatures at different thicknesses.
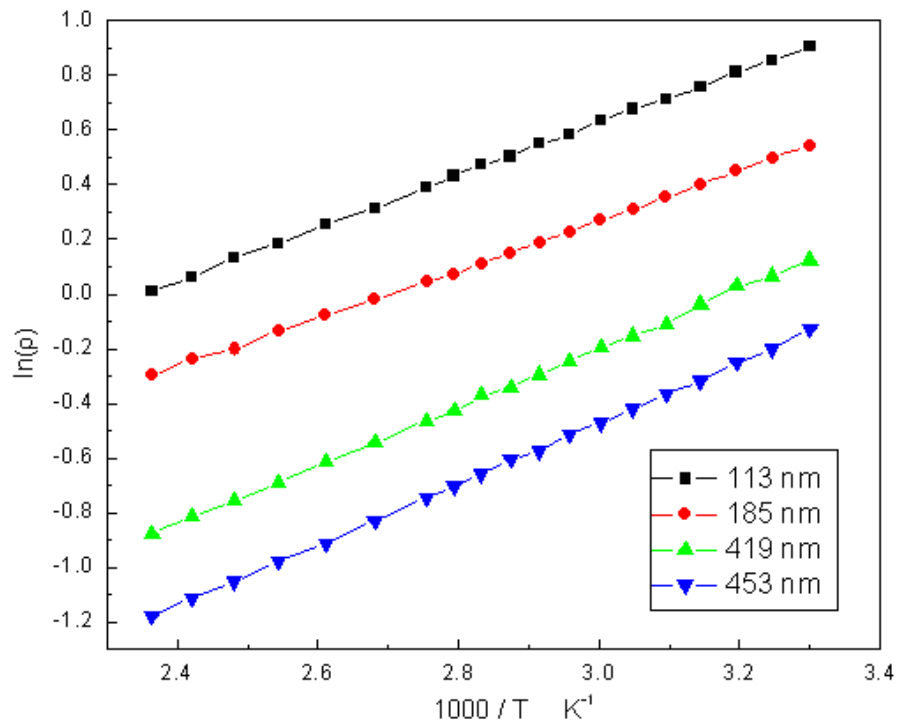

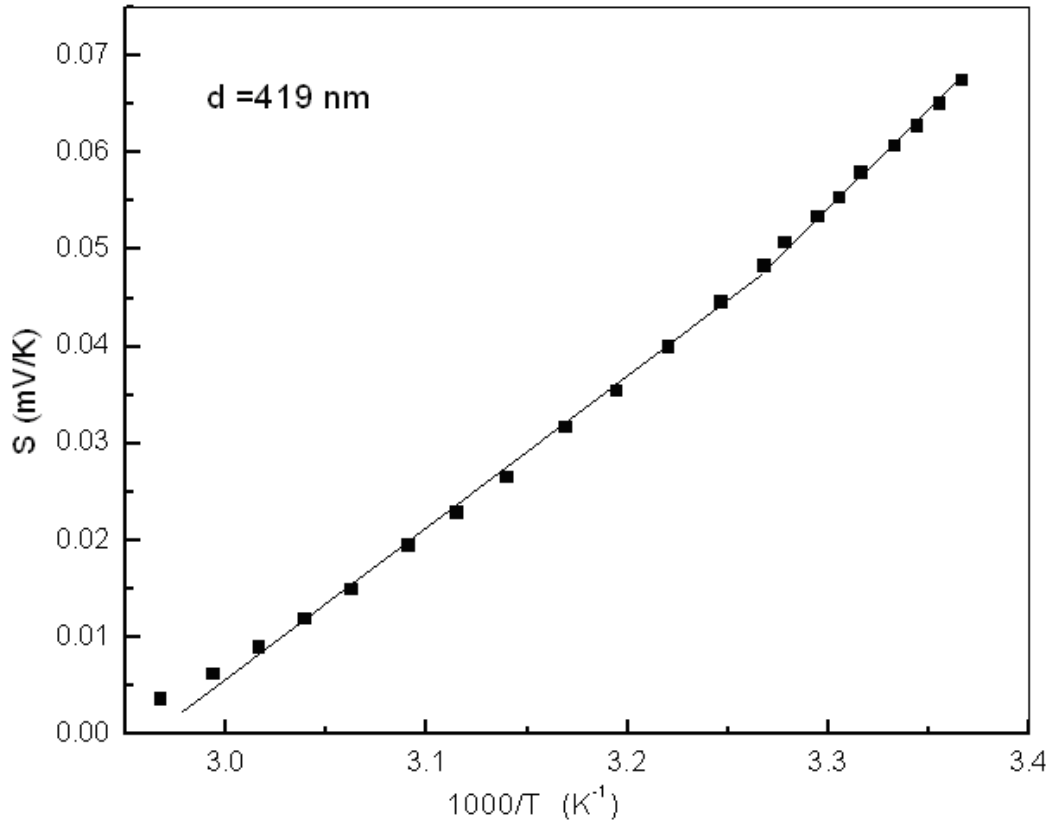Fig.12. ln(ρ) Vs 1000/T of Cu_2S films at different thicknesses.

Fig.13. S Vs 1000/T of Cu$_2$S films.

The film resistivity decreasing as the increasing of film thickness and annealing temperature is attributed to the improvement of crystallite size (Shaaban *et al*., 2009).

The thickness dependence of electrical resistivity of Cu$_2$S films considering the surface scattering of charge carriers was analyzed (Sondheimer, 1952; Kimr, 2000). A simple analytical expression for the electrical resistivity as a function of thickness is considered. According to this model, the film resistivity is simply given by (Tellier, 1987):

$$\rho = \rho_B \ [1+3l_o \ (1\text{-}p)/8d] \tag{3}$$

Where ρ_B is the electrical resistivity of the infinite thick film and named bulk resistivity, l_o is the mean free path and *p* is the proportion of electron scattering that is elastic. Assuming that all scattering at film boundaries is inelastic (p = 0), Eq.3. becomes as follows:

$$\rho.d = \rho_B.d +(3/8)l_o \ \rho_B \tag{4}$$

The values for the bulk resistivity and mean free path can be obtained by plotting the relation between ρ.d versus d as shown in figure10. The graph shows straight lines at different temperatures. The slope gives the bulk resistivity, ρ_B and from the intercept the mean free path, l_o, can be determined for different temperatures. The calculated values are listed in table 2.

Table 2. Annealing effect on bulk resistivity and mean free path of Cu$_2$S films.

Temperature (K)	Bulk resistivity ,ρ_B, (Ω.cm)	Mean free path (μm)
303	0.46	1.33
323	0.33	1.60
343	0.24	1.91
363	0.19	2.11
383	0.16	2.26
403	0.13	2.46
423	0.11	2.60

The temperature dependence of resistivity is expressed as follows (Mott and Davis, 1971; Dongol *et al*., 2000):

$$\rho = \rho_o \ \exp \ (\Delta E/k_B T) \tag{5}$$

Where ρ_o is a constant, ΔE is the activation energy of the free charge carriers, and k_B is the Boltzmann's constant. The variation of ρ versus temperature at different film thicknesses is illustrated in figure 11. It is observed that for each film thickness, the dark resistivity decreases with the increasing of annealing temperature. ΔE could be determined by plotting   ln ρ Vs 1000/T at different thicknesses as depicted in figure 12. The corresponding

activation energies are calculated and listed in table 3. The obtained data agree with the findings characters of (Abdullaev *et al*., 1968; Sorokin and Paradenko, 1966). The observed changes was attributed to the enhancement of crystallite size consequently the structural changes.

Table 3. Thickness effect on the activation energy of Cu_2S films.

Film thickness (nm)	Activation energy (eV)
113	0.08
185	0.084
419	0.092
453	0.096

The thermoelectric power of Cu_2S thin film of thickness 419 nm has been studied.

The temperature dependence of *S* in case of p-type semiconductors is given by (Mott and Davis, 1971; Dongol *et al*., 2007).

$$S = \frac{k_B}{|e|}\left(\frac{\Delta E_s}{k_B T} + A\right) \dots\dots\dots(6)$$

where ΔE_s is the activation energy, *e* is the electronic charge, K_B Boltzmann constant, T is the absolute temperature and A is a constant represent the thermal energy transported by the carriers. Its magnitude is dependent on the nature of the scattering processes, the values of ΔE_s and the constant *A* can be obtained using the slope and the intercept of Eq.6. $\Delta E_s = E_F - E_v$; E_F is Fermi level energy and E_v is the energy at the top of the valence band. The temperature dependence of the thermoelectric power (*S*) of as deposited films is illustrated in figure 13. It was found that *S* is always positive indicating the p-type nature of the Cu_2S films. The slope of the straight line of Eq.6 yields $\Delta E_S = 20$ meV which represent the energy difference between Fermi level and top of the valence band due to that Cu_2S is P-type. The linearity of S as a function of temperature, suggested that the Cu_2S is a degenerate semiconductor (Dongol *et al*., 2007; Shahane and Deshmukh, 2001).

CONCLUSION

Different thicknesses of Cu_2S films were prepared by thermal evaporation technique. The EDX analysis of the as deposited thin has stoichiometric structure and the chemical formula of the compound is $Cu_{1.96}$ S. XRD of Cu_2S indicated that the material in thin film form is nano structure characterized by polycrystalline in nature with orthorhombic crystal system. Lattice parameters: *a* = 11.82 A, b= 27.05 A and *c* = 13.43 A°. The SEM of the as-deposited Cu_2S thin film shows uniform formation of the film and clearly indicates the formation of nano

crystalline structure with crystallite size range (12-420 nm). The AFM of the as-deposited Cu_2S thin film shows that both average size and roughness increases by annealing. The dark electrical resistivity measured for Cu_2S thin films was found to decrease with increasing the film thickness. The bulk resistivity and the mean free path are determined for different temperatures. The temperature dependence of dark electrical resistivity showed a semiconductor behavior. The conduction type was investigated using the thermoelectric power, which showed that Cu_2S is p-type semiconductor material.

REFERENCES

Abdel Rafea, M., Farag, AAM. and Roushdy, N. 2012. Controlling the crystallite size and influence of the film thickness on the optical and electrical characteristics of nanocrystalline Cu_2S films. Materials Research Bulletin. 47:257-266.

Abdullaev, GB., Aliyarovea, A., Zamanova, H. and Asadov, GA. 1968. Investigation of the electric properties of Cu2S single crystals. Phys. stat. sol. 26:65-68.

Carvalho, CN., Parreira, P., Lavareda, G., Brogueira, P. and Amaral, A. 2013. P-type Cu_xS thin films: Integration in a thin film transistor structure. Thin Solid Films. 543:3-6.

Dhumure, SS. and Lokhands, CD. 1992. Preparation and characterization of chemically deposited Ag_2S films. Sol. Energy Mater. Sol. Cells. 28:159-166.

Dongol, M., Abou Zied, M., Gamal, GA. and El-Denglawey, A. 2000. Effects of copper content and heat treatment on the electrical properties of $Ge_{15}Te_{85-x}Cu_x$ thin films. Appl. Surf. Sci. 161:365-374.

Dongol, M., El-Nahass, MM., El-Denglawey, A., Elhady, AF. and Abuelwafa, AA. 2012[a]. Optical Properties of Nano 5, 10, 15, 20-Tetraphenyl-21H, 23H-Porphine Nickel (II) thin films. Current Applied Physics. 12:1178-1184.

Dongol, M., El-Nahass, MM., El-Denglawey, A., Elhady, AF. and Abuelwafa, AA. 2012[b]. Structural Properties of Nano 5, 10, 15, 20-Tetraphenyl-21H, 23H-Porphine Nickel (II) thin films. Current Applied Physics. 12:1334-1339.

Dongol, M., El-Nahass, MM., Abou-zied, M. and El-Denglawey, A. 2007. Thermoelectric properties and mobility activation energy of amorphous $As_{20}Se_{80-x}Tl_x$ films. Eur. Phys. J. Appl. Phys. 37:257-260.

ELdenglawy, A. 2005. A study of Electrical, Optical and Structure Properties of AS-Se-TI Thin Film". Ph.D. Thesis. South Valley University.

Grozdanove, I. and Najdoski, M. 1995. Optical and Electrical Properties of Copper Sulfide Films of Variable Composition. J. Solid State Chem. 114:469-475.

Kamazani, MM., Niasari, MS. and Sadeghinia, M. 2013. Synthesis and characterization of Cu_2S nanostructures via cyclic microwave radiation. Superlattices and Microstructures. 63:248-257.

Kimr, IH. 2000. Electronic transport properties of the flash-evaporated p-type $Bi_{0.5}Sb_{1.5}Te_3$ thermoelectric thin films. Mater. Lett. 44:75-79.

Lewkowicz, A., Synak, A., Grobelna, B., Bojarski, P., Bogdanowicz, R., Karczewski, J., Szczodrowski, K. and Behrendt, M. 2014. Thickness and structure change of titanium(IV) oxide thin films synthesized by the sol‑gel spin coating method. Opt. Mater. 36:1739-1744.

Li, DM., Cheng, LY., Zhang, YD., Zhang, QX., Huang, XM., Luo, YH. and BoMeng, Q. 2014. Development of Cu_2S/carbon composite electrode for CdS/CdSe quantum dot sensitized solar cell modules. Solar Energy Materials and Solar Cells. 120:454-461.

Li, J., Zhao, H., Chen, X., Jia, H. and Zheng, Z. 2013. In situ fabricate Cu_2S thin film with hierarchical petal-like nanostructures. Materials Research Bulletin. 48:2940-2943.

Mott, NF. and Davis, EA. 1971. Electronic Process in Non- Crystalline Materials. Clarendon Press, Oxford. 236-238.

Ohtani, T., Motoki, M., Koh, K. and K. Ohshima. 1995. Synthesis of binary copper chalcogenides by mechanical alloying. Materials Research Bulletin. 30:1495-1504.

Salim, NT., Yamada, M., Nakano, H., Shima, K., Isago, H. and Fukumoto, M. 2011. The effect of post-treatments on the powder morphology of titanium dioxide (TiO_2) powders synthesized for cold spray. Surface and Coatings Technology. 206:366-371.

Shaaban, ER., Afify, N. and A. El-Taher. 2009. Effect of film thickness on microstructure parameters and optical constants of CdTe thin films. J. Alloys Compds. 482:400-404.

Shahane, GS. and Deshmukh, LP. 2001. Structural and electrical transport properties of $CdS_{0.9}Se_{0.1}$: in thin films: effect of film thickness. Mater. Chem. Phys. 70:112-116.

Shinde, MS., Ahirrao, PB., Patil, IJ., Disawal, SK. and Patil, RS. 2013. Current voltage characteristics modeling of polycrystalline CdTe-CdS solar cells for different grain-sizes of CdTe. IJNEAM. 6:29-35.

Sondheimer, EH. 1952. The mean free path of electrons in metals. Adv. Phys. 1:1-42.

Sorokin, GP. and Paradenko, AP. 1966. Electrical properties of Cu_2S. Soviet Phys. I. 9: 59-61.

Su, CY., Mishra, DK., Chiu, CY. and Ting, JM. 2013. Effects of Cu_2S sintering aid on the formation of $CuInS_2$ coatings from single crystal $Cu_2In_2O_5$ nanoparticles. Surface and Coatings Technology. 231:517-520.

Tellier, CR. 1987. A theoretical description of grain boundary electron scattering by an effective mean free path. Thin Solid Films. 51:311-317.

Tolansky, S. 1988. Multiple Beam Interferometry Surfaces and Films, Oxford, London. 147-148.

Varin, RA., Bystrzycki, J. and Calka, A. 1999. Effect of annealing on the microstructure, ordering and microhardness of ball milled cubic (L12) titanium trialuminide intermetallic powder. Intermetallics. 7:785-796.